14th IEA Heat Pump Conference
15-18 May 2023, Chicago, Illinois

Development of a Near-isothermal Compressor for Transcritical Carbon Dioxide Cycle

Cheng-Yi Lee, Timothy Kim, Jan Muehlbauer, Yunho Hwang*,

Reinhard Radermacher

Center for Environmental Energy Engineering
Department of Mechanical Engineering, University of Maryland,
4164 Glenn Martin Hall Bldg., College Park, MD 20742, United States

Abstract

This study demonstrates the feasibility of a near-isothermal compressor for the transcritical CO_2 compression cycle. A copper tube-based compression chamber was designed, built, and installed in the open-loop liquid piston compression system. The oil compressed the CO_2 in the chamber from 40°C, 4,000 kPa to 10,000 kPa by an external gear pump. A 59% isothermal compression efficiency was measured at 900 RPM motor speed. To increase the efficiency, we tried the following two options: (1) lower the operation speed and (2) enhance the heat transfer rate. Evaporative cooling was applied by installing a mist generator in front of the chamber to improve the outer heat transfer performance. According to the experimental results, simply slowing down the operation to 270 RPM increases the efficiency to 80%, and combining evaporative cooling and slower operation delivers 93.8% of isothermal efficiency. Under this enhancement, the compression power can be 30% less than the isentropic compression. Several suggestions have been proposed to improve the current prototype's performance.

Keywords: Isothermal compression; Trans-critical CO2; Efficiency; Heat pump; Refrigeration

1. Introduction

The transcritical CO_2 application has been getting much attention recently, considering it has numerous advantages over traditional HFC refrigerants. First, CO_2 refrigerant is much cheaper than the HFC or HFO system. Second, CO_2 is a natural refrigerant with a global warming potential of 1, which will not be regulated. Hence, many researchers in academia and industry have considered CO_2 as a long-term solution for approaching carbon neutrality. Many applications are being studied and investigated, including vehicle heat pumps, residential heat pumps, heat pump water heaters, heat pump dryers, and commercial refrigeration [1].

Many methods can improve the efficiency of the transcritical CO_2 system, such as optimizing the gas cooler design, improving the control logic through artificial intelligence, or recovering the expansion work by using an expander, ejector, vortex tube, and so on. One of the intriguing approaches is reducing the compression work through isothermal compression. It can be commonly seen in Compressed Air Energy Storage (CAES) for isothermal compression technology to reduce the work required for compression, increasing the charge-discharge efficiency for CAES [2]. Unlike these conventional approaches, we proposed an integrated gas cooler compression system combining the gas cooler and compression chamber. In the typical transcritical CO_2 system, refrigerants are compressed isentropically, carrying the compression work to the gas cooler. Then the compression work and inherent internal energy are discharged into the environment. So the refrigerant enthalpy can reach the designed conditions. This study integrates these two processes into a single isothermal compression process, compressing the refrigerant and discharging the heat simultaneously and isothermally to

* Corresponding author. Tel.: +1-301-405-5247
E-mail address: yhhwang@umd.edu.

improve the system's efficiency. This work demonstrates the suggested idea's feasibility and proposes future design improvement suggestions.

2. Isothermal and Isentropic Compression in Transcritical CO_2

The transcritical CO_2 near-isothermal compression demonstrated excellent potential for compression work reduction and is compared with the isentropic compression process using the property chart in EES (Engineering Equation Solver). In Figure 1, the red square symboled curve illustrates the CO_2 refrigerant being isentropically compressed from 40°C and 4,000 kPa inlet to 10,000 kPa outlet. It should be noted that this suction condition is after considering the suction line heat exchanger to be employed. For isentropic compression, the compression work is the enthalpy difference between the initial and final state, which follows the isentropic line in the P-h diagram. On the contrary, the compression work of isothermal compression includes heat discharged out of the compression chamber to keep the constant compression temperature. Hence, the isothermal compression work could not be shown in the P-h diagram but can be evaluated in another way as follows. First, the isothermal compression process is divided into many finite segments. As an example, 100 segments are shown in Figure 1. Each segment comprises an isentropic compression and an isobaric cooling along the isothermal line. Then the isothermal compression work was derived by integrating the tiny consecutive compression and cooling operation for 100 segments. The other way is to integrate the pressure and volume variation during the compression process, as shown in Eq. (1).

$$W = \int_{V_i}^{V_f} P dV = \int_{V_i}^{V_f} \frac{ZnRT}{V} dV = ZnRTln\frac{V_f}{V_i} \quad (1)$$

where Z is the compressibility factor.

By comparing the finite segments approach with the ideal gas law approach, the calculated work difference is only 0.2%. Since pressure and temperature sensors are installed in the system, the refrigerant status can be calculated immediately and reflected in the P-h diagram. Therefore, the finite segments method would be applied to the following calculation to facilitate the compression work estimation.

Table 1. Compression Work Comparison

Initial Compression Conditions	Final Compression Condition	Isothermal Compression Work	Isentropic Compression Work	Work Reduction
40°C, 4,000 kPa	10,000 kPa	32.9 kJ/kg	48.5 kJ/kg	32.1 %

Table 1 illustrates the work input requirement to compress the CO_2 refrigerant from 40°C, 4,000 kPa to 10,000 kPa isothermally or isentropically. The isothermal compression work is 32.9 kJ/kg, and the isentropic compression work is 48.5 kJ/kg. Therefore, if the isothermal compression process replaces the isentropic compression in transcritical CO_2, the overall potential work reduction can achieve 32.1%, which benefits the refrigeration industry by cutting off the carbon footprint. The following chapter explains how this study experimentally approaches the near-isothermal process and demonstrates the possible work reduction using this technology.

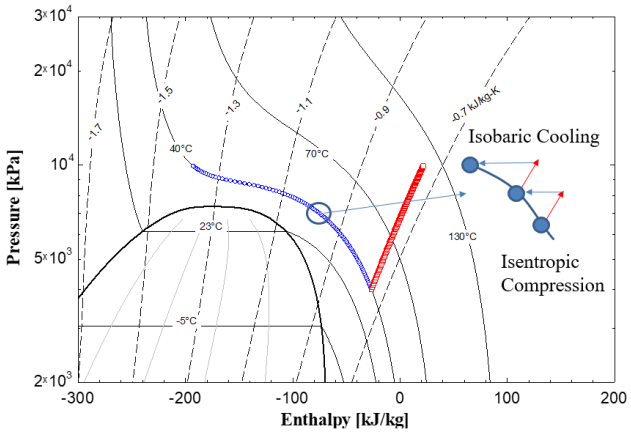

Fig. 1. CO_2 Compression Processes in P-h Diagram

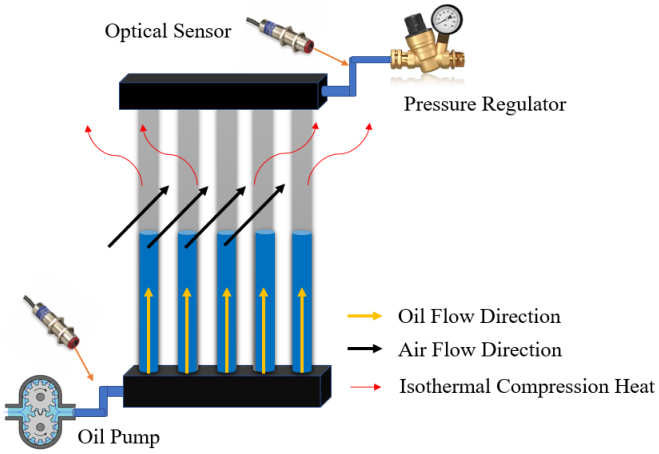

Fig. 2. Isothermal Compression Mechanism Schematic Diagram

3. Experimental Facility

3.1. Isothermal Compression Process Mechanism

A simple figure illustrating the fluids' movement was created to give the readers a better understanding of how we approach near-isothermal compression. In Figure 2, the CO_2 refrigerant stored in the compression chamber was compressed by pressurized oil, and the CO_2 pressure increased when the oil level elevated. Meanwhile, forced air cooling discharged the CO2 compression work and its internal energy from the compression chamber, maintaining the isothermal process. Once the CO_2 pressure reached the designed pressure, the pressure regulator opened, and the compressed CO2 was delivered downstream. The compression process finished when the upper optical sensor detected the oil level.

3.2. Experimental Facility

The first open-loop liquid piston isothermal compressor prototype has been designed for CO_2 and built to demonstrate the near-isothermal compression process, as shown in Figure 3 and the actual picture in Figure 4. The dimensions of the experimental facility, including integrated gas cooler compression chamber, tube diameters, and gear pump capacities, were developed based on delivering 1.75 kW of cooling capacity. Therefore, the self-built compression chamber utilized 17 of 6.2 mm inner diameter copper tubes with an outer diameter of 9.5 mm. The 1.65 mm wall thickness was designed to have a working pressure of 16,500 kPa and a burst pressure of 25,000 kPa with a safety factor of 1.5. The overall dimensions of the chamber are 0.61 m wide and 0.55 m height. And the overall heat transfer area is 0.279 m^2. The detailed chamber design parameters are listed in Table 2.

Table 2. Chamber Design Parameters

Parameter	Unit	Value
Compressor Suction Temperature	°C	40
Evaporating Temperature	°C	5
Mass Flow Rate	g/s	13.3
Cooling Capacity	kW	1.75
Operating Pressure	kPa	4,000 - 10,000
Cycle Frequency	Hz	0.1
Chamber Volume	m^3	0.00117
Chamber Heat Transfer Area	m^2	0.279

In Figure 3, the experimental facility is categorized into three major sections: (1) The left-hand side liquid oil circulation section. (2) The integrated gas cooler compression chamber. (3) The right-hand side compressed CO_2 storage and release section. At the beginning of the compression process, the mineral oil was fed into the 9.5 c.c gear pump at a given driven speed from the open oil tank. The atmosphere pressure oil was compressed

to 11,000 kPa limited by a back pressure regulator to ensure the liquid piston pressure was large enough to compress CO_2 to 10,000 kPa. In parallel, there is a relief valve set to 12,000 kPa for its bypass back to the oil tank in case of any unexpected situation. Since the gear pump operated continuously, even not in the compression process, the friction loss would increase the oil temperature. Before entering the compression chamber, an oil heat exchanger was placed to prevent heat accumulation and maintain the constant oil temperature. Two solenoid valves break down the liquid piston cycle into compression and suction process. If the compression solenoid valve opens and the suction solenoid closes, the oil flows into the compression chamber and starts compressing, and if the compression solenoid closes and the suction solenoid opens, the oil flows back to the oil tank. The compression speed depends on the driving speed of the motor. On the other hand, the suction speed depends on the opening of the needle valves. The longer the suction time, the more accurate the replenishment mass flow rate would be, but it reduced the cycle frequency or cooling capacity.

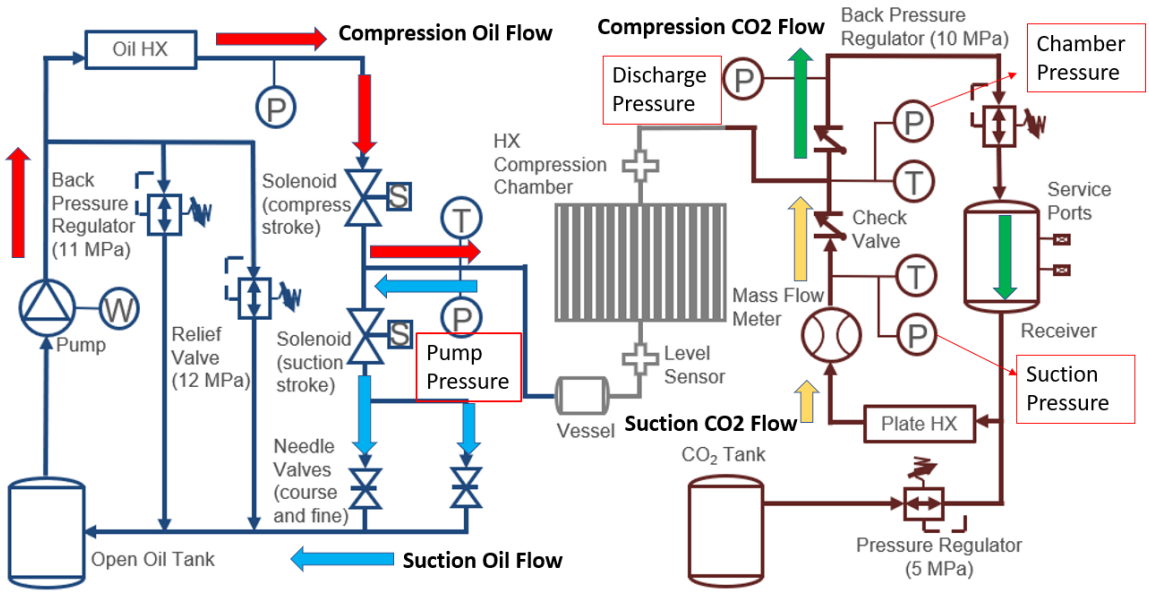

Fig. 3. Experimental Facility Schematic Diagram

The aforementioned integrated gas cooler compression chamber is located in the middle of the facility. The system's criteria for deciding when to compress and release depends on two optical leveling sensors. When the dyed mineral oil passes through the bottom-level sensors during the suction process, the detected sensor signal change makes the compression solenoid open, the suction solenoid close, and the compression process starts. When the oil reaches the top of the level sensor, the system responds vice versa.

Upon reaching 10,000 kPa for the CO_2 refrigerant compression, the compressed CO_2 passes the upper back pressure regulator and enters the receiver. During the suction process, a certain amount of CO2 was degassed from the mineral oil because of the solubility difference between 10,000 kPa and atmosphere pressure. Hence, the CO_2 from the supply tank would compensate for this loss and be mixed with CO_2 from the receiver. Altogether, the mixed CO_2 was conditioned to 40°C and recorded by the mass flow meter before flowing back into the compression chamber.

3.3. Instruments and Uncertainties

Table 3 lists the experimental facility's instruments and their systematic error. All the instruments were calibrated before being installed in the facility. The data were acquired when the system operated for at least half an hour and reached a steady state.

Table 3. Instruments and Uncertainties

Instrument	Model	Range	Systematic Error
Pressure Transducer	Setra, 280E	0 – 20,684 kPa	± 0.11% FS
RTD	Omega, 1/10 DIN	-100 °C – 400 °C	± 1/10 x (0.3 + 0.005 x t) °C
Mass Flow Meter	Micromotion CMFS010M	0 – 30 g/s	± 0.25% of reading
Watt Meter	Ohio Semitronics, PC5-062D	0 – 10 kW	± 0.5% F.S.
Gear Pump	Honor Externa,l 2GG1U09R	9.5 c.c. per rev.	N.A.
Motor	Baldor, EJMM.401T	10 hp, 1770 RPM max.	N.A
Axial Fan	N.A	1000 CFM	N.A

3.4 Test Matrix

The experimental facility was built inside the environmental chamber, which was set at 35°C and 20% in humidity. The initial chamber's temperature and pressure were set to 40 °C and 4000 kPa, respectively. And the final chamber pressure is 10,000 kPa. Two pump speeds, 270 RPM and 900 RPM have been chosen. In addition to the fan cooling, the room-temperature water mist was sprayed on the compression chamber surface as a heat transfer enhancement method in test #3, and an additional fan was installed to facilitate the water evaporation.

Table 4. Test Matrix

Test Number	Initial Chamber Temperature °C	Initial Chamber Pressure kPa	Final Chamber Pressure kPa	Pump Speed RPM	Evaporative Cooling Mist Temperature °C	Axial Fan Number
#1	40	4,000	10,000	900	NA	1
#2	40	4,000	10,000	270	NA	1
#3	40	4,000	10,000	270	35	2

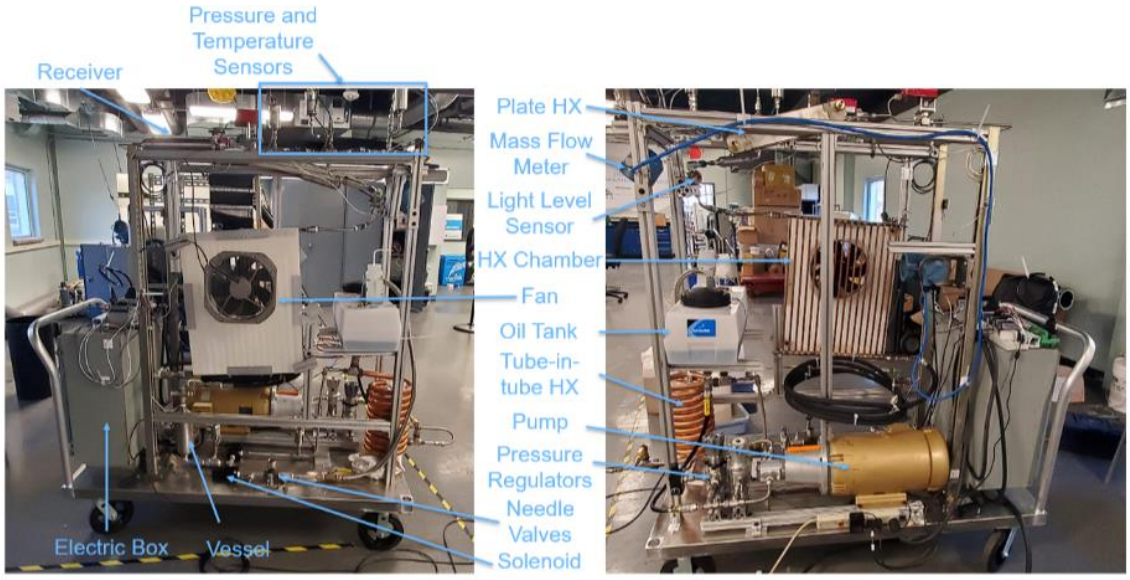

Fig. 4. Picture of Compression Chamber (left) and Experimental Facility (right)

4. Results and Discussion

4.1. 900 RPM Operation with Axial Fan Cooling: Test #1

The motor operation speed of 900 RPM has been chosen to observe the compression chamber's temperature and pressure variation under the isothermal compression process. In Figure 4, the upper graph displays the pressure variation in each measuring section. When the compression process starts, the pump elevates the liquid piston and compresses the refrigerant in the chamber, increasing the pump and chamber pressure simultaneously. Once the chamber pressure reaches 10,000 kPa, the upper back pressure regulator opens, and the compressed CO_2 flows into the receiver, which causes the suction pressure to increase. After the oil level reaches the upper-level sensors, the solenoid valves are switched, and the suction process is started. Consequently, the pump pressure built up because the compression solenoid valve closed, and the chamber started to decompress to the initial conditions (40°C, 4,000 kPa) and then started the compression process over again.

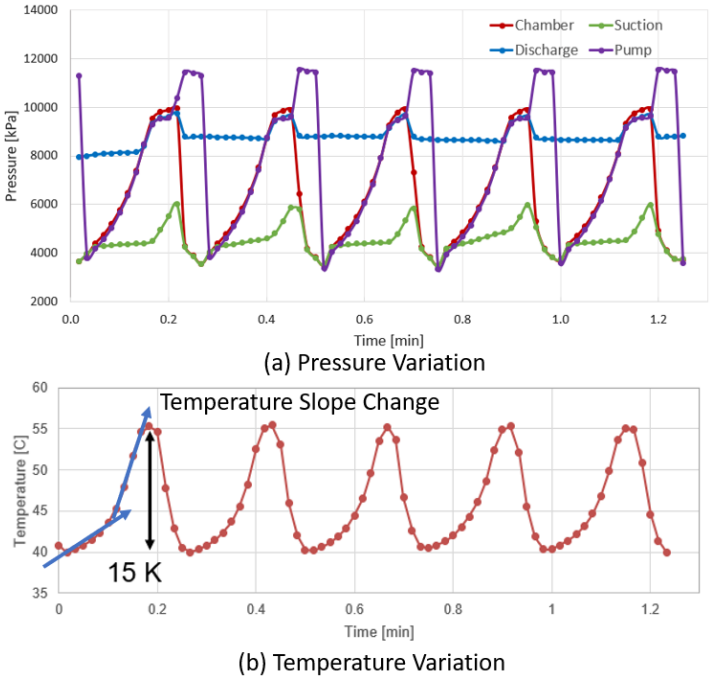

Fig. 4. Pressure and Temperature versus Time Plot at 900 RPM

Compared with the isentropic compression, which would result in a 117°C chamber temperature under the same given conditions, the current temperature increased to 55°C with a 15 K lift, demonstrating a 62 K temperature suppression. The chamber temperature in Figure 4 describes this temperature suppression for the test #1 condition. One thing worth noting is that the temperature curve has a noticeable slope change at around 7,000 kPa. It can be attributed to heat transfer area reduction and the reaching of the local CO_2 pseudocritical point. First, the heat transfer area between the compressed CO_2 and the environment becomes less as the liquid oil level upraises during compression. Second, Figure 5 shows that CO_2 density and specific heat increased dramatically from 4,000 kPa to 10,000 kPa, which means the internal energy is significantly different. The same thing can be observed in the P-h diagram, shown in Figure 1. A significant enthalpy drop can be found along the 40°C isothermal line. These factors make the chamber temperature inevitably deviate from the isothermal process.

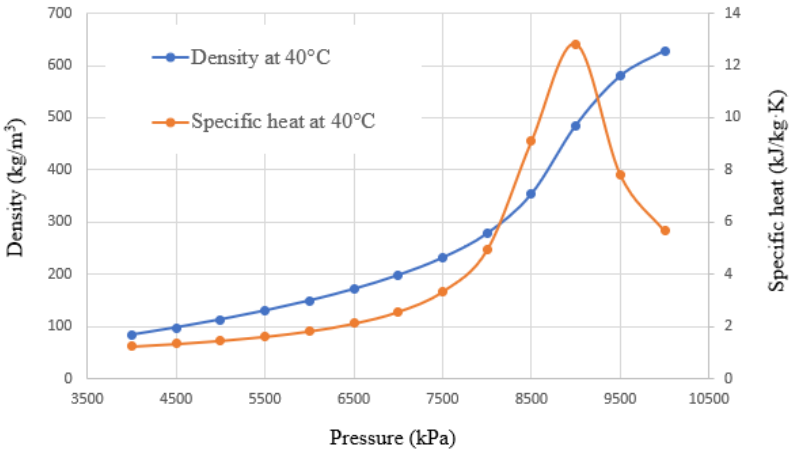

Fig. 5. Density and Specific Heat of CO_2 at 40°C and Various Pressures

The compression power curve and the mass flow rate of replenished CO_2 are depicted in Figure 6. Due to the open-loop design, the gear pump has to consume energy to hold the pump pressure to 4,000 kPa from atmospheric pressure, corresponding to the power consumption below the black line, which is about 1 kW. The motor power can be derived by integrating along the power line above the black line. According to the given product specification, the gear pump and motor have a combined efficiency of 0.72, and the actual work input for compressing the CO_2 must consider this factor. At the bottom of Figure 6, refrigerant replenishment can be derived by integrating the mass flow rate curve, and the integrated value stands for the initial CO_2 mass stored in the chamber for the next compression cycle.

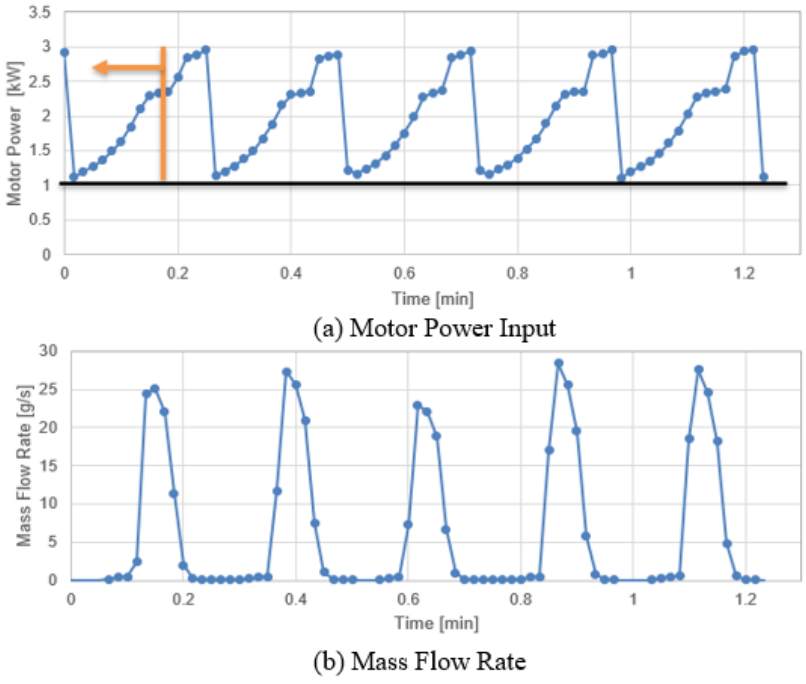

Fig. 6. Motor Power Input and CO_2 Mass Flow Rate

4.2. 270 RPM Operation and Evaporative Cooling Heat Transfer Enhancement: Tests #2 and 3

Based on the experimental results from the 900 RPM operation, which has 59.7% of isothermal efficiency, the current chamber design was too small to approach the near-isothermal operation for 1.75 kW cooling capacity. Nevertheless, the near-isothermal operation is still achievable by manipulating the control operation and heat transfer enhancement.

First, the motor compression speed is decreased to 270 RPM, the minimum allowable operating speed for the installed gear pump (Test #2). By slowing down the compression process, the extended heat transfer time helps discharge the accumulated heat inside the compression chamber. In contrast to Figures 5 and 6, Figure 7 only focuses on the single compression stroke. As shown in the upper left of Figure 7, the temperature lift is reduced to 10.6 K compared to 15 K in 900 RPM operation. For evaluating how the entire process is close to the isothermal compression, isothermal efficiency is defined as the ideal isothermal compression work divided by the actual compression work, which can be found in Eq. (2). And the motor plus pump efficiency was defined as actual compression work divided by the integrated work from the measurement, as shown in Eq. (3).

$$\eta_{iso} = \frac{W_{isothermal}}{W_{actual}} = \frac{Mass_{chamber} \cdot w_{isothermal}}{W_{integrated} \cdot \eta_{motor+pump}} \tag{2}$$

$$\eta_{motor+pump} = \frac{W_{actual\ work}}{W_{integrated\ work}} \tag{3}$$

In Eq. (2), the $W_{isothermal}$ represents the ideal compression work for the amount of CO_2 in the compression chamber, which was the product of CO_2 mass and the specific ideal isothermal work. The CO_2 mass can be derived from the initial CO_2 density and chamber volume. And $w_{isothermal}$ is the specific ideal isothermal work calculated from the second section, 32.9 kJ/kg. The actual work is calculated from the integrated work multiplied by the efficiency of the motor and pump. A 59.7 % isothermal efficiency can be found for operating the system at 900 RPM. As a comparison, a significant improvement to 80% isothermal efficiency can be achieved by slowing down the pump speed to 270 RPM.

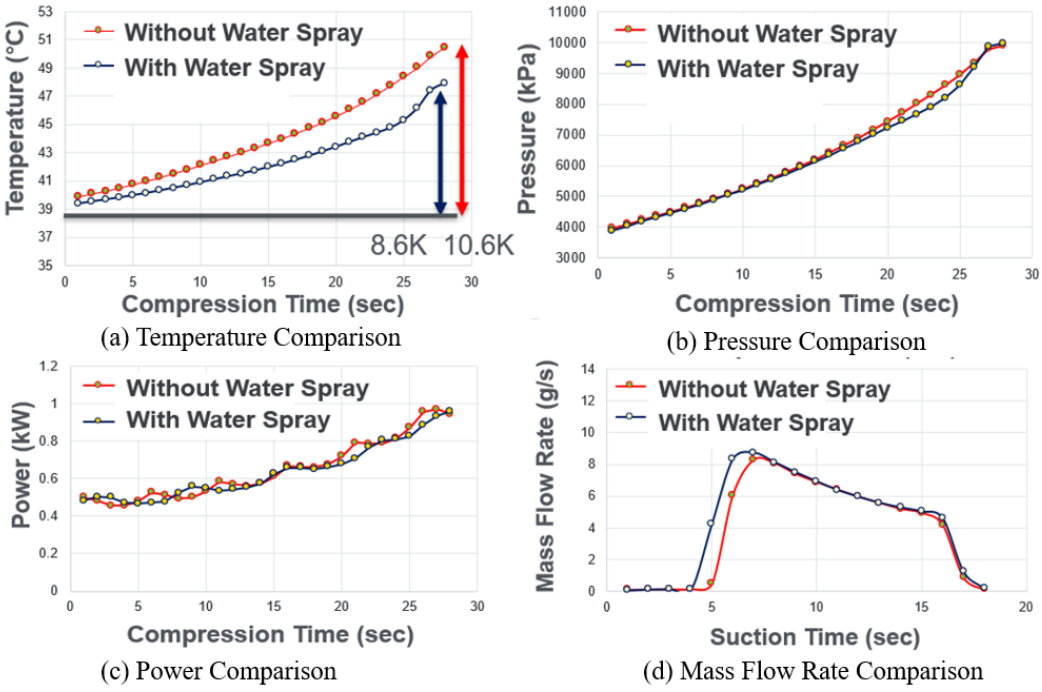

Fig. 7. Compression Behaviour Comparison at 270 RPM

Except for slowing down the rotation speed, additional heat transfer enhancement can be applied to the integrated gas cooler compression chamber (Test #3). While the current chamber's configuration limited the improvement method, evaporative cooling was chosen to help further enhance the heat transfer. According to Heyns and Kroger (2010), the water film heat transfer coefficient ranges from 1,500 to 3,000 $W/m^2 \cdot K$, which is the function of the deluge water mass flow rate, air mass flow rate, and deluge water temperature. The enhancement can significantly reduce the thermal resistance at the outer surface. Hence, a water mist generator was placed in front of the compression chamber. We made sure all the tubes were sufficiently wet during the compression chamber. In addition, one more axial fan was installed to improve the air volumetric flow rate, helping the water evaporate from the tube surface. By doing so, the temperature curve in Figure 7 shows further temperature suppression and maintains a relatively low-temperature increase compared to test #2. In the upper right of Figure 7, the pressure shows an evident suppression from 7,000 to 9,000 kPa, which has the most heat needed to be removed in the entire process.

However, a rapid increase in temperature and pressure occurred around 9,000 to 10,000 kPa because the heat transfer area was still too small to discharge heat. Evaporative cooling effectively improves the heat transfer rate and isothermal efficiency, which results in a 93.8% achievement. A detailed comparison can be found in Table 5. However, the lower motor RPM results in a decrease in cooling capacity. Assuming a gas cooler and a suction line heat exchanger were installed in the system, the cooling capacity in each test would be 1719, 674, and 743 W, respectively.

Table 5. Compression Performance Comparison

Objective	Unit	900 RPM	270 RPM	270 RPM with Evaporative Cooling
Energy per Cycle	kJ	6.12	3.91	3.67
Initial CO_2 Density	kg/m^3	84	83	81
CO_2 in Chamber	g	107	106	103.5
$W_{isothermal}/W_{actual}$	%	59.7	80.0	93.8
Average CO_2 Mass Flow Rate	g/s	7.4	2.9	3.2
Cooling Capacity	W	1719	674	743

Although the demonstrated prototype achieved high isothermal efficiency, many future design opportunities can improve furthermore. First, water has become scarce as climate change exacerbates yearly, and using it as heat transfer enhancement is not the ideal option. Instead, different geometries or fins would be applied to the outer compression chamber to increase the heat transfer area and coefficient. Second, the preliminary thermal resistance analysis shows that the CO_2 side was the dominant contributor to the overall thermal resistance compared with the conduction resistance and external resistance. Therefore, the heat transfer enhancement technique should also be applied to the internal chamber to lower the thermal resistance. Third, due to the lower operation speed, the average CO_2 mass flow rate was much lower than the design capacity. The number of tubes for the compression chamber should be increased accordingly to increase the heat transfer area and cooling capacity

5. Conclusions

The prototype of a near-isothermal compressor for transcritical CO_2 has been built and demonstrated the capability of achieving high isothermal efficiency. In this study, a 0.61 m by 0.55 m integrated gas cooler compression chamber was self-built, utilizing 17 tubes in 9.5 mm diameter. The compression process was set to compress 40°C, 4,000 kPa CO_2 to 10,000 kPa. Three different operation conditions were performed and compared: (1) 900 RPM compression with fan cooling, (2) 270 RPM compression with fan cooling, and (3) 270 RPM compression with evaporative cooling. The demonstrated isothermal efficiency was 59.7%, 80%, and 93.8%, respectively. Based on the current experimental results, three main improvement options were suggested: (1) enhance the outer heat transfer area and geometry of the compression chamber, (2) improve the inner heat transfer rate by applying turbulators or internal fins, and (3) increase the number of such tubes to enable a faster compression speed for higher system capacity. This study demonstrated that the near-isothermal compression process could be achieved. The 93.8% isothermal efficiency contributes 30% of the compression power input savings compared to traditional isentropic compression, which may facilitate the world and industry to achieve net-zero emissions.

Acknowledgments

This work was supported by the United States Department of Energy Award Number DE-EE0009685, the Consortium for Energy Efficiency and Heat Pumps, and the Center for Environmental Energy Engineering (CEEE) at the University of Maryland.

References

[1] Song, Y., Cui, C., Yin, X., & Cao, F. (2022). Advanced development and application of transcritical CO2 refrigeration and heat pump technology—A review. Energy Reports, 8, 7840-7869.
[2] Kim, T., Lee, C. Y., Hwang, Y., & Radermacher, R. (2022). A review on nearly isothermal compression technology. International Journal of Refrigeration.
[3] Heyns, J. A., & Kröger, D. G. (2010). Experimental investigation into the thermal-flow performance characteristics of an evaporative cooler. Applied Thermal Engineering, 30(5), 492-498.